

Performance of Automotive Fuel Cell Systems with Nanostructured Thin Film Catalysts

R. Ahluwalia¹, X. Wang¹, S. Lasher², J. Sinha², Y. Yang², S. Sriramulu²

¹Argonne National Laboratory, Argonne, IL

²TIAX LLC, Cambridge, MA

Introduction

Cost and durability are generally regarded as the major challenges to commercialization of fuel cells. Size, weight, and system complexity are also important barriers to adoption of fuel cells in light duty vehicles. In addition, thermal and water management for fuel cells are outstanding issues. Fuel cell operation at lower temperatures creates a small difference between the operating and ambient temperatures, necessitating large heat exchangers. Fuel and air feed streams need to be humidified for proper operation of fuel cells. Whereas having to carry consumable water on-board the vehicle is considered unacceptable, recovering water formed in the fuel cell adds to the system complexity. In this paper, we evaluate the prospects of overcoming the barriers of cost, durability, weight, volume, thermal management, and water management by using nanostructured thin film (NSTF) catalysts in membrane electrode assemblies (MEA). In laboratory tests, the NSTF catalysts have shown significantly enhanced stability against surface area loss from Pt dissolution when compared to conventional Pt/C dispersed catalysts under both accelerated voltage cycling from 0.6 to 1.2 V and real-time start stop cycles. Also, NSTF catalyst support-whiskers have shown total resistance to corrosion when held at potentials up to 1.5 V for 3 h [1].

Fuel Cell System Performance

Figure 1 is a schematic of an idealized 80-kW_e system in which the polymer electrolyte fuel cell (PEFC) stack operates at 2.5 atm at rated power, 50% O₂ utilization and 70% per-pass H₂ utilization. The MEA consists of NSTF ternary-Pt catalysts supported on organic whiskers, a modified perfluorosulfonic acid (PFSA) membrane and gas diffusion layers made from woven carbon fibers. The flow channels are fabricated from 2-mm-thick expanded graphite plates, with each plate having cooling channels in it. The air management subsystem consists of a compressor-expander module (CEM) with a liquid-cooled motor, mixed axial and radial flow compressor, variable-nozzle radial inflow turbine, and airfoil bearings. The fuel management subsystem includes a hybrid ejector-hydrogen pump to recirculate a portion of the spent anode gas. The water management subsystem uses an enthalpy wheel humidifier (EWH) for the cathode feed and a membrane humidifier (MH) for the anode feed. The system is designed to be water balanced, i.e., only the water produced in the stack is used for humidifying the feed gases. The dual-loop heat rejection subsystem has a high-temperature circuit for supplying coolant to the stack and a low-temperature circuit for supplying coolant at 55°C to the vehicle traction motor and the CEM motor. The coolant in both circuits is aqueous ethylene glycol solution.

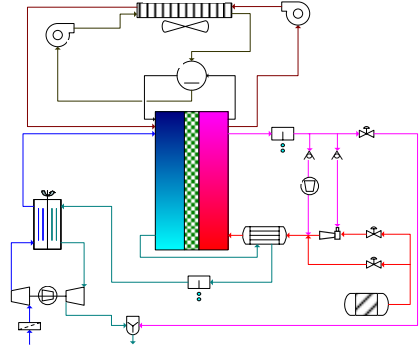


Figure 2 shows the modeled polarization curve of a stack with the NSTF catalyst, based on 185 mA/mg-Pt mass activity and of 2.85 mA/cm²-Pt specific activity at 0.9 V (IR corrected, 1-atm O₂ partial pressure, 100% RH, 80°C) for a ternary Pt/Co_x/Mn_y alloy with Pt to transition metal ratio of 3:1 and Pt loading of 0.2 mg/cm² [2]. The polarization curve is for a 30-μm-thick 3M membrane, that with stabilizing additives and a reduced number of carboxylic end groups, has exhibited good oxidative stability in load cycling tests at 90°C for >4000 h [4]. The NSTF catalyst (0.3 mg/cm² total Pt loading) is supported on organic whiskers that are assumed to have 5x10⁹/cm² area number density, 1-μm height, and 50-nm diameter. Consistent with the experimental data, our model

indicates that the relative humidity (RH) of the feed streams must be controlled to prevent flooding of the thin film catalysts or membrane dry-out. Figure 3 shows the optimum cathode stoichiometry (SR) and RH of the cathode air at stack inlet as a function of the current density normalized with respect to the current density at rated power (1.1 A/cm^2 at 0.684 V and 2.5 bar , 750 mW/cm^2 power density). The optimum conditions at part load have been determined from the compressor operating map, water mass transfer in the enthalpy wheel humidifier and the membrane humidifier, and the stack polarization curves for different pressures, anode/cathode inlet RH, and anode/cathode SR. Figure 3 indicates that because of the increase in cathode RH with the decrease in current density (i.e., mass flow rate), the cathode SR must be raised in order to prevent flooding of the thin film catalysts at part load conditions. At the optimum operating conditions, the spent gases at the stack outlet are just saturated, although liquid water does form in the catalyst layers. The higher operating temperature (90°C vs. 80°C) and the lower inlet RH (50% vs. 60%) imply that the stack with the NSTF catalyst runs much drier than the stack with the dispersed catalyst, and the problems of water management in the gas diffusion layers and the flow fields are considerably reduced.

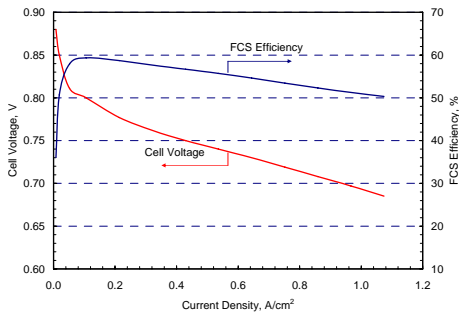


Figure 2. Stack and system performance.

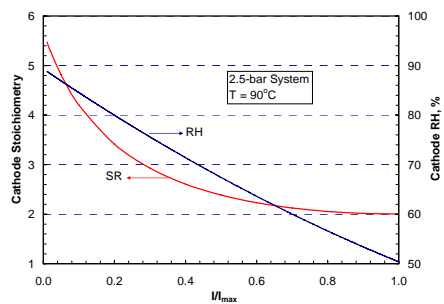


Figure 3. Stack operating conditions.

Heat rejection is more challenging when driving on grade than at the top speed because of the smaller amount of ram air available at the lower speed. We have looked at the possibility of making the radiator more compact by allowing the stack temperature to rise while driving on grade. Our results indicate that the cathode SR must be reduced from the optimum value shown in Fig. 3 if the stack temperature is allowed to rise; otherwise, the membrane dries out, the stack efficiency decreases, and more waste heat has to be rejected. Compared to an ICE for the same vehicle platform, a 20–30% larger frontal area is needed for the radiator if the stack temperature is allowed to rise to $92\text{--}98^\circ\text{C}$ while driving on grade. Although the FCS radiator is considerably larger than its ICE counterpart, it is still significantly more compact than the radiator needed for a stack with the dispersed Pt catalyst that operates at 80°C .

High Volume Manufacturing Cost

We have estimated the cost of manufacturing the 80-kW_e FCS at a high production volume of 50,000 units/year. A bottom-up approach was used to determine the cost of the major stack and balance-of-plant components. We used experience-based estimates for components such as stack sensors and control and power electronics. A vertically integrated manufacturing process was used for the stack; consequently, the cost projections do not include supplier markups for such components as the MEA and bipolar plates. Also excluded was the cost of stack conditioning and testing since these requirements are still evolving.

A “cast dispersion” process of preparing the membrane was constructed from the available literature on forming non-reinforced PFSA membranes [3]. The cost of manufacturing the membrane was estimated assuming a coater-laminator line with a line rate of 20 ft/min . The 1.2-mil ($30 \mu\text{m}$) membrane needs only a single pass to complete the coating process, which leads to lower failure rate (20% machine downtime) and higher yield (95%) assumptions. The estimated membrane cost on an active area basis is $\$16/\text{m}^2$, 87% of which is due to the materials.

We assumed that roll good catalyst layers are fabricated by vapor depositing perylene red on an aluminum-coated film substrate and vacuum annealing it to form an organic whisker layer [4]. A vacuum sputtering process is used to coat the catalyst materials (Pt, Co and Mn) onto the organic whiskers, followed by laminating with Teflon sheets. Assuming \$35.4/g cost for Pt and 10% conversion cost, the estimated cost on an active area basis is \$41/m² for the anode catalyst layer (0.1 mg/cm² Pt loading) and \$79/m² for the cathode catalyst layer (0.2 mg/cm² Pt loading). More than 90% of the cost of the electrodes is due to the materials.

In constructing a manufacturing process flow for the gas diffusion layers, it was assumed that woven carbon cloth is available as un-coated rolls [3]. The process includes steps for applying PTFE to increase the hydrophobicity of the carbon fibers to avoid flooding. The estimated cost of the GDLs on an active area basis is \$13/m², about 89% of which is in materials.

The process flow for the expanded graphite foil bipolar plates is based on a Graftech® process chart and related patents [3]. It is assumed that expanded graphite flakes are prepared in a high-temperature exfoliation furnace and are available at \$2/lb. The manufacturing process consists of roll pressing the expanded graphite flakes into flexible foil, resin impregnation, calendaring, emboss compression molding, die cutting, and curing. We estimate that the expanded graphite foil bipolar plate cost is \$18/m², of which material costs represent about 57%.

We have assumed that transfer molding is used to fabricate the seals between the MEA and the bipolar plate. The seal material is Viton® that costs about \$20/lb. The estimated cost of the gaskets is \$9/m², of which \$5/m² is for materials.

A process flow chart was constructed to assemble MEAs from catalyst layers, membrane, GDLs and seals. It was assumed that the anode and cathode organic whisker layers are hot pressed to the membrane with Teflon backing sheets. The catalyst coated membrane and GDLs are laminated to form an MEA in roll good form. The MEA is then die-cut into sheets and molded with a frame seal. The MEA and frame seal cost is estimated to be \$158/m², of which the MEA cost is \$149/m².

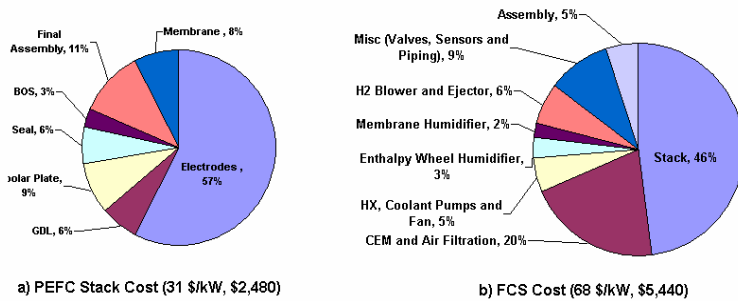


Figure 4. Projected cost at high volume manufacturing.

A robotic press concept was developed to assemble stacks from compression molded bipolar plates, transfer molded gaskets, MEAs with frame seals and balance of stack components. The stack assembly cost of \$23/m² includes quality control but not stack conditioning. We estimate that the stack with the NSTF catalyst will cost \$2,480 for the 80-kW_e FCS or \$31/kW_e. Figure 4a indicates that the electrodes represent approximately 57% of the stack cost. The membrane, GDLs, bipolar plates, seals and final assembly are other significant contributors to the cost of the PEFC stack.

We are also doing bottom-up costing for the major BOP sub-systems, namely thermal management, water management, air management and fuel management. Since several of the BOP components are not produced at high volumes or they are not amenable to continuous manufacturing processes, their contribution to the overall system cost is significant. It is assumed that the BOP components are purchased from suppliers; therefore, markups are included in the cost of these components. The

total estimated cost of the BOP components in the 80-kW_e FCS is \$2,960 or \$37/kW_e; this estimate includes previous estimates for the air and fuel management, which are being updated with bottom-up costing. Figure 4b provides a breakdown of the BOP cost and shows that the air management subsystem makes the largest contribution to the BOP cost.

The total estimated cost of the 80-kW_e FCS at high volume production is \$5,440 or \$68/kW_e. The PEFC stack accounts for 46% of the total system cost (excluding stack conditioning cost and OEM markups).

Summary and Conclusions

Table 1 summarizes the important performance and cost attributes of the 80-kW_e FCS with the NSTF catalyst and compares them with results from a previous study with dispersed Pt catalysts. Also included are the corresponding 2010 DOE targets for automotive fuel cell systems. The following are some major conclusions from this study.

- At 0.3 mg/cm² total Pt content in ternary NSTF catalysts, it is possible to reach a stack power density of 750 mW/cm² at a cell voltage needed for 50% system efficiency at rated power.
- Water management and heat rejection are considerably simplified with the use of NSTF catalysts that operate drier and allow the stack temperature to exceed 90°C under infrequent driving conditions.
- With high volume manufacturing, the projected cost of the PEFC stack with NSTF catalyst is \$31/kW_e, exclusive of the cost of stack conditioning and manufacturer's markups.
- The total projected cost of 80-kW_e FCS is \$68/kW_e at high volume manufacturing. The BOP components and stack contribute equally to the total cost.

Table 1. Performance and cost summary

	Units	NSTFC-FCS	2010 Target
System Cost	\$/kW _e	68	45
System Efficiency @ 25% Rated Power	%	60	60
System Efficiency @ Rated Power	%	50	50
System Specific Power	W/kg	790	650
System Power Density	W/L	640	650
Stack Cost	\$/kW _e	30	30
Stack Efficiency @ 25% Rated Power	%	62	65
Stack Efficiency @ Rated Power	%	55	55
Stack Specific Power	W/kg	1900	2000
Stack Power Density	W/L	2070	2000
MEA Cost	\$/kW _e	21	15
MEA Performance @ Rated Power	mW/cm ²	740	1280
MEA Degradation Over Lifetime	%	TBD	10
PGM Cost	\$/kW _e	16	8
PGM Content (peak)	g/kW _e	0.4	0.5
PGM Loading (both electrodes)	mg/cm ²	0.3	0.3
Membrane Cost	\$/m ²	16	40
Bipolar Plate Cost	\$/kW _e	3	6
CEM System Cost	\$	1080	400

Acknowledgements

This work was supported by the U.S. Department of Energy's Office of Energy Efficiency and Renewable Energy, Office of Hydrogen, Fuel Cells, and Infrastructure Technologies.

References

1. M. K. Debe, S. J. Hamrock, and R. T. Atanoski, "Advanced MEAs for Enhanced Operating Conditions," FY 2006 Annual Progress Report, DOE Hydrogen Program, pp. 692-697, November 2006.
2. A. K. Schmoeckel, et al, "NanoStructured Thin Film Ternary Catalyst Activities for Oxygen Reduction," 2006 Fuel Cell Seminar, Honolulu, HI, Nov. 13-17, 2006.
3. E. J. Carlson, P. Kopf, J. Sinha, S. Sriramulu, and Y. Yang, "Cost Analysis of PEM Fuel Cell Systems for Transportation," NREL/SR-560-39104, Dec. 2005.
4. M. K. Debe, et al, "Nanostructured Thin Film Catalysts for PEM Fuel Cells for Vacuum Web Coating," 50th Annual Technical Conference of the Society of Vacuum Coaters, Louisville, KY, May 1, 2007.